A novel method to aging state recognition of viscoelastic sandwich structures

Jinxiu Qu [1a], Zhousuo Zhang [*1], Xue Luo [1], Bing Li [1] and Jinpeng Wen [2]

[1] *State Key Laboratory for Manufacturing Systems Engineering,*
Xi'an Jiaotong University, Xi'an 710049, People's Republic of China
[2] *Institute of Systems Engineering, China Academy of Engineering Physics,*
Mianyang 621999, People's Republic of China

Abstract.   Viscoelastic sandwich structures (VSSs) are widely used in mechanical equipment, but in the service process, they always suffer from aging which affect the whole performance of equipment. Therefore, aging state recognition of VSSs is significant to monitor structural state and ensure the reliability of equipment. However, non-stationary vibration response signals and weak state change characteristics make this task challenging. This paper proposes a novel method for this task based on adaptive second generation wavelet packet transform (ASGWPT) and multiwavelet support vector machine (MWSVM). For obtaining sensitive feature parameters to different structural aging states, the ASGWPT, its wavelet function can adaptively match the frequency spectrum characteristics of inspected vibration response signal, is developed to process the vibration response signals for energy feature extraction. With the aim to improve the classification performance of SVM, based on the kernel method of SVM and multiwavelet theory, multiwavelet kernel functions are constructed, and then MWSVM is developed to classify the different aging states. In order to demonstrate the effectiveness of the proposed method, different aging states of a VSS are created through the hot oxygen accelerated aging of viscoelastic material. The application results show that the proposed method can accurately and automatically recognize the different structural aging states and act as a promising approach to aging state recognition of VSSs. Furthermore, the capability of ASGWPT in processing the vibration response signals for feature extraction is validated by the comparisons with conventional second generation wavelet packet transform, and the performance of MWSVM in classifying the structural aging states is validated by the comparisons with traditional wavelet support vector machine.

Keywords: viscoelastic sandwich structures; aging state recognition; vibration response signals; adaptive second generation wavelet packet transform; multiwavelet support vector machine

1. Introduction

Viscoelastic sandwich structures (VSSs) are the composite structures in which viscoelastic layers are sandwiched between steel layers (Moita *et al.* 2011, Bilasse *et al.* 2011). Because of the perfect performance in energy dissipation, VSSs are playing an important role in sealing, vibration

∗Corresponding author, Professor, E-mail: zzs@mail.xjtu.edu.cn
[a] Ph.D. Student, E-mail: xjtuqjx@stu.xjtu.edu.cn
[b] Ph.D., E-mail: zzs@mail.xjtu.edu.cn

damping and noise reduction of mechanical equipment. During the long-term service of VSSs, their health states are influenced by such environmental factors and their variations as temperature and humidity, and hence structural aging will come up inevitably. The main reason resulting in the structural aging is the aging of viscoelastic material. If aging occurs, the dynamic characteristics of VSSs may be forced to change, which will result in the performance degradation of VSSs and even lead to the breakdown of the entire mechanical equipment. Moreover, huge financial loss and even serious personal injury maybe unfortunately caused, if VSSs keep servicing in an excessive aging state and timely maintenance is not performed. Consequently, to ensure the usability and reliability of VSSs, it is urgent to study on the aging state recognition method which can recognize the structural aging states accurately and automatically.

Aging can be regarded as a kind of damage that affects the performance of VSSs, and aging state recognition of VSSs belongs to the scope of structural health monitoring. Owing to the advantages of convenience, efficiency and non-destruction, vibration response analysis is one of the principal tools widely applied in the scope of structural health monitoring (Carden and Fanning 2004, Yan *et al*. 2007, Fan and Qiao 2011, Hou *et al*. 2012, Xiang *et al*. 2012, Sun *et al*. 2014a, Xiang *et al*. 2014, Qu *et al*. 2014, Xiang *et al*. 2015, Zhang *et al*. 2016). As an important carrier of structural state information, vibration response signals generated by different structural aging states tend to vary. By performing some processing techniques on vibration response signals, vital state information can be obtained from the vibration response signals. Moreover, aging state recognition of VSSs, through the vibration response analysis, can be treated as a problem of pattern recognition. It consists of three steps: data acquisition, feature extraction, and state classification. Feature extraction is the key of aging state recognition, and state classification is the core of aging state recognition. However, due to the strong non-stationarity of vibration response signals and the weakness of state change characteristics, it is difficult to carry out the two tasks of feature extraction and state classification effectively. For this reason, in order to make the accurate and automated aging state recognition of VSSs come true, it is of great significance to develop effective feature extraction and state classification means.

The purpose of feature extraction is to extract features representing the structural aging states to be used for state classification. However, due to the high nonlinearity on the dynamic characteristics of VSSs, the measured vibration response signals are strongly non-stationary so that the useful state information is usually too weak to be extracted from the raw vibration response signals. Thus, in order to obtain contributing state information, it is essential to employ effective signal processing techniques to analyze the vibration response signals before feature extraction. Wavelet transform (WT), possessing the property of multi-resolution analysis, has been proven to be highly powerful in non-stationary mechanical signal analysis for feature extraction (Peng and Chu 2004, Yan *et al*. 2014, Si *et al*. 2015, Meng *et al*. 2015a). Subsequently, second generation wavelet transform (SGWT) is presented by Sweldens (1998) using lifting scheme in time domain. Compared with classical WT, SGWT possesses such advantages as simple, fast, irregular samples and integral transform. What is more important is that SGWT provides much more flexibility and freedom for the construction of biorthogonal wavelets and can achieve adaptive wavelet construction via the design of prediction operator and update operator. Second generation wavelet packet transform (SGWPT) is an extension of SGWT, and overcomes the shortcoming that SGWT cannot realize multi-resolution analysis in the high frequency band where the contributing state information always exists (Leng *et al*. 2007, Hu *et al*. 2007, Pan *et al*. 2009, Meng *et al*. 2015b). However, one common approach taken by SGWPT is that, the wavelet is constructed via the design of prediction operator and update operator by means of equivalent filter method (Claypoole

2003). Unfortunately, such wavelet functions constructed via this method are fixed and independent of the vibration response signal of VSSs. In practice, the measured vibration response signal is relevant to the structural aging state and different structural aging states will result in various vibration response signals. Therefore, for aging state recognition of VSSs, inappropriate wavelets irrelevant to the input vibration response signals are harmful to feature extraction and hence reduce the accuracy of state classification. In order to overcome this shortcoming, based on the time domain characteristics of given vibration response signal, Qu *et al*. (2014) proposed an adaptive second generation wavelet construction method and applied it to looseness state recognition of VSSs. However, when the VSS is in different aging states, the frequency spectrum and its distribution of the vibration response signal are different too. In this paper, to obtain sensitive feature information to the different structural aging states, a novel adaptive second generation wavelet construction method is firstly proposed based on the frequency spectrum characteristics of inspected vibration response signal. Then, adaptive second generation wavelet packet transform (ASGWPT) which can realize multi-resolution analysis in the whole frequency band is developed to process the vibration response signals for feature extraction. Finally, energy in each frequency band of reconstructed wavelet packet coefficients is extracted and taken as the feature to describe the structural aging states.

After the feature extraction based on ASGWPT, state classification is another task in aging state recognition of VSSs. State classification via intelligent techniques can provide an automated aging state recognition procedure. Support vector machine (SVM), presented by Vapnik (2000), is a state of the art intelligent technique based on statistical learning theory and structural risk minimization principle. Due to its strong generalization ability even when the training samples are few, the SVM has been used in many applications for classification purpose. However, the generalization ability of SVM depends heavily on the used kernel function that maps the input data into a higher dimensional feature space where the data can be linearly separated. Currently, the most commonly adopted kernel function is Gaussian kernel. Over the past decade, the kernel function research of SVM has received substantial attention from scholars in many application fields. Zhang *et al*. (2004) proposed wavelet support vector machine (WSVM) by constructing scalar wavelet kernel on the basis of the kernel method of SVM and wavelet theory, and proved that the WSVM outperforms the traditional SVM in the application field of classification. For the past few years, successful implementations of WSVM have been emerged in the mechanical fault diagnosis (Keskes *et al*. 2013, Liu *et al*. 2013, Chen *et al*. 2013) and looseness state recognition of VSSs (Qu *et al*. 2014). However, a set of bases in the square and integrable space, constructed through the translations and dilations of a single wavelet function, cannot have orthogonality, symmetry, short support and high order vanishing moments at the same time (Daubechies 1992). Therefore, the approximation performance of scalar wavelet kernel is limited, which affects the classification performance of WSVM. With multiple wavelet functions, multiwavelets possess orthogonality, symmetry, short support and high order vanishing moments simultaneously (Sun *et al*. 2014b, Chen *et al*. 2015). Thus, a set of bases in the square and integrable space, constructed through the translations and dilations of multiwavelet functions, can overcome the above mentioned difficulty. In this paper, for further improving the generalization ability of SVM in classifying the different aging states of VSSs, based on the kernel method of SVM and multiwavelet theory, multiwavelet functions are used to construct the new SVM kernel function named multiwavelet kernel, and then multiwavelet support vector machine (MWSVM) is developed. Multiwavelets have more advantages than scalar wavelets do, so the MWSVM can obtain the higher state classification accuracy than the WSVM does.

Based on the above principles, in order to accurately and automatically recognize the aging state of VSSs, a novel aging state recognition method based on ASGWPT and MWSVM is proposed in this paper. In this method, for extracting sensitive feature information to different structural aging states, based on the frequency spectrum characteristics of inspected vibration response signal, the ASGWPT is developed to adaptively process the vibration response signal in the whole frequency band, and then energy features are extracted from the frequency bands of reconstructed wavelet packet coefficients to reflect the aging state of VSSs. In order to achieve desired state classification accuracy, as a combination of SVM and multiwavelet theory, the MWSVM is developed to automatically classify the different aging states of VSSs by using the extracted energy features as the input features.

The rest of this paper is organized as follows. In Section 2, a brief review of SGWT is firstly given and then adaptive second generation wavelet construction method is proposed. Finally, ASGWPT is developed for feature extraction. In Section 3, summaries of SVM and multiwavelets are firstly given. Then, multiwavelet functions are adopted to construct multiwavelet kernel functions for SVM. Lastly, MWSVM is developed for state classification. The proposed aging state recognition method for VSSs is presented in Section 4. In Sections 5, the proposed aging state recognition method is performed on the experimental case to demonstrate its performance. Conclusions are given in Section 6.

2. Adaptive second generation wavelet packet transform and feature extraction

When the aging state of VSSs changes, the frequency spectrum and its distribution of the corresponding vibration response signal change too. From this point, for extracting sensitive feature information to the change of structural aging state, a feature extraction method based on ASGWPT is proposed in this section. Firstly, adaptive second generation wavelet is constructed based on the frequency spectrum characteristics of inspected vibration response signal. Then, in order to realize multi-resolution analysis in the whole frequency band, ASGWPT is developed for feature extraction, and energy in each frequency band of reconstructed wavelet packet coefficients is computed and taken as the feature to describe the structural aging state.

2.1 Review of second generation wavelet transform

In order to bring about the development of ASGWPT, a brief review of SGWT is firstly given in this section. The decomposition stage of SGWT mainly consists of the following three steps (Sweldens 1998).

In the split step, the original signal x is divided into even samples x_e and odd samples x_o.

$$x_e(k) = x(2k), \qquad x_o(k) = x(2k+1), \qquad k \in Z \tag{1}$$

In the predict step, we apply an operator P on even samples x_e to predict odd samples x_o. The prediction error d is regarded as the detail coefficients of x.

$$\boldsymbol{d} = \boldsymbol{x}_o - \boldsymbol{P}(\boldsymbol{x}_e) \tag{2}$$

where $P = [p_1, p_2, ..., p_N]$ is defined as prediction operator, and N is the number of prediction coefficients.
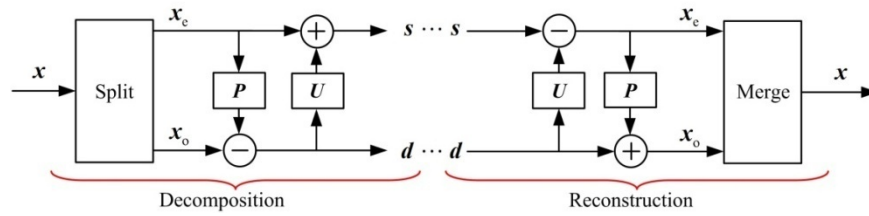
Fig. 1 The decomposition and reconstruction stages of SGWT

In the update step, an operator U is applied on the detail coefficients d to update even samples x_e. By adding the result to x_e, the update sequence s is considered as the approximation coefficients of x.

$$s = x_e + U(d) \tag{3}$$

where $U = [u_1, u_2, ..., u_{\widetilde{N}}]$ is defined as update operator, and $\widetilde{N}$ is the number of update coefficients.

By performing the above three steps on the approximation coefficients s, the detail and approximation coefficients at the lower resolution level can be obtained. The reconstruction stage of SGWT is the inverse of the decomposition stage, and can be immediately performed by reversing the prediction operator and update operator and changing each '+' into '−' and vice versa. The decomposition and reconstruction stages of SGWT are shown in Fig. 1.

2.2 Construction of adaptive second generation wavelet

Due to not relying on the Fourier transform, SGWT can achieve adaptive wavelet construction by the design of prediction operator and update operator. Based on the time domain characteristics of inspected vibration response signal, an adaptive second generation wavelet construction method is proposed in our previous work (Qu *et al*. 2014), and the design process of prediction operator and update operator was discussed in detail. In this paper, on the basis of the publication (Qu *et al*. 2014), a new adaptive second generation wavelet construction method is proposed to ensure that the wavelet function can closely match the frequency spectrum characteristics of given vibration response signal.

2.2.1 Design of prediction operator

It can be seen in Fig. 1 that, the prediction operator P is used to generate the detail coefficients d. In order to make the designed prediction operator can effectively separate feature components from the original vibration response signal, an evaluation index for guiding the optimal design of prediction operator is required. Shannon entropy, as an effective measure to represent the diversity of probability distribution, is widely applied to optimization principles (Kapur and Kesavan 1992). Therefore, the minimum entropy principle is recommended to seek for the optimal prediction operator, by means of measuring the sparsity. Moreover, when the VSS is in different aging states, the frequency spectrum and its distribution of the vibration response signal may change. Consequently, the frequency spectrum entropy of the detail coefficients d is chosen as the evaluation index to guide the optimal design of prediction operator P in this paper.

If $\{f_i\}$ is the frequency spectrum of the detail coefficients $\{d_i\}$, calculate the probability density function $p(f_i)$. Define the frequency spectrum entropy as follows

$$E_f = -\sum_i^n p(f_i)\ln p(f_i) \tag{4}$$

Our objective is to obtain the optimal prediction operator P_{opt} by finding the minimum value of frequency spectrum entropy E_f, and the specific implementation process can be seen in the publication (Qu *et al.* 2014).

2.2.2 Design of update operator

It can also be seen in Fig. 1 that, using the optimal prediction operator P_{opt} designed above, the detail coefficients can be obtained, and then the update operator U is applied on these detail coefficients to produce the approximate coefficients at a lower resolution. In order to ensure that the produced approximation coefficients can provide an accurate representation of the original vibration response signal at the lower resolution, an evaluation index for guiding the optimal design of update operator is also needed. In this paper, the quadratic error of reconstruction without using the detail coefficients is chosen as the evaluation index to guide the optimal design of update operator U.

Our objective is to obtain the optimal update operator U_{opt} by solving the minimum value of the quadratic error, and the detailed optimal design procedure can be seen in the publications (Gouze *et al.* 2004, Li *et al.* 2008, Qu *et al.* 2014).

On the basis of the above designed optimal prediction operator P_{opt} and optimal update operator U_{opt}, adaptive second generation wavelet which can adaptively match the frequency spectrum characteristics of inspected vibration response signal can be constructed.

2.3 Adaptive second generation wavelet packet transform for feature extraction

Construction of adaptive second generation wavelet can get the better effect on the feature extraction from complex vibration response signals. Furthermore, in order to realize multi-resolution analysis in the whole frequency band, ASGWPT is developed based on the constructed adaptive second generation wavelet. Compared with traditional SGWPT, ASGWPT is a more precise signal processing method because its wavelet function can adaptively match the frequency spectrum characteristics of inspected vibration response signal. The decomposition and reconstruction stages of ASGWPT are expressed as below.

In the decomposition stage, $c_{l,k}$ is split into even samples $c_{l,ke}$ and odd samples $c_{l,ko}$,

$$c_{l,ke} = c_{l,k}(2i), \quad c_{l,ko} = c_{l,k}(2i+1) \tag{5}$$

where $c_{l,k}$ represent the wavelet packet coefficients of the kth frequency band at level l. The wavelet packet coefficients of the each frequency band at level $l + 1$ are calculated as follows

$$\begin{cases} c_{l+1,2} = c_{l,1o} - P_{opt}(c_{l,1e}) \\ c_{l+1,1} = c_{l,1e} + U_{opt}(c_{l+1,2}) \\ \quad \cdots \\ c_{l+1,2^{l+1}} = c_{l,2^l o} - P_{opt}(c_{l,2^l e}) \\ c_{l+1,2^{l+1}-1} = c_{l,2^l e} + U_{opt}(c_{l+1,2^{l+1}}) \end{cases} \tag{6}$$

where P_{opt} is the designed optimal prediction operator and employed on even samples $c_{l,2^l\,\mathrm{e}}$ to predict odd samples $c_{l,ko}$, and the prediction error $c_{l+2^{l+1}}$ is considered as the wavelet packet coefficients of the 2^{l+1}th frequency band at level $l + 1$. U_{opt} is the designed optimal update operator and employed on the wavelet packet coefficients $c_{l+2^{l+1}}$ to update even samples $c_{l,2^l\,\mathrm{e}}$, by adding the result to $c_{l,2^l\,\mathrm{e}},$, the update sequence $c_{l+2^{l+1}-1}$ is considered as the wavelet packet coefficients of the $(2^{l+1} - 1)$th frequency band at level $l + 1$.

The reconstruction stage of ASGWPT can be deduced from its decomposition stage. In this paper, the frequency-band signals of decomposition stage are individually reconstructed to obtain the detailed description of original signal. With regard to the individual reconstruction of a frequency-band signal, the wavelet packet coefficients of the frequency band to be reconstructed are reserved, and the wavelet packet coefficients of other frequency bands are set to be zeroes. Finally, the reconstructed results are obtained as follows

$$
\begin{cases}
c_{l,2^l\,\mathrm{e}} = c_{l+1,2^{l+1}-1} - U_{opt}\left(c_{l+1,2^{l+1}}\right) \\
c_{l,2^l\,\mathrm{o}} = c_{l+1,2^{l+1}} + P_{opt}\left(c_{l,2^l\,\mathrm{e}}\right) \\
c_{l,2^l}\left(2i\right) = c_{l,2^l\,\mathrm{e}} \\
c_{l,2^l}\left(2i+1\right) = c_{l,2^l\,\mathrm{o}} \\
\qquad\cdots \\
c_{l,1\mathrm{e}} = c_{l+1,1} - U_{opt}\left(c_{l+1,2}\right) \\
c_{l,1\mathrm{o}} = c_{l+1,2} + P_{opt}\left(c_{l,1\mathrm{e}}\right) \\
c_{l,1}\left(2i\right) = c_{l,1\mathrm{e}} \\
c_{l,1}\left(2i+1\right) = c_{l,1\mathrm{o}}
\end{cases}
\tag{7}
$$

The decomposition and reconstruction stages of ASGWPT are displayed in Fig. 2. It should be noted that ASGWPT can decompose a signal into independent frequency bands with equal frequency widths.
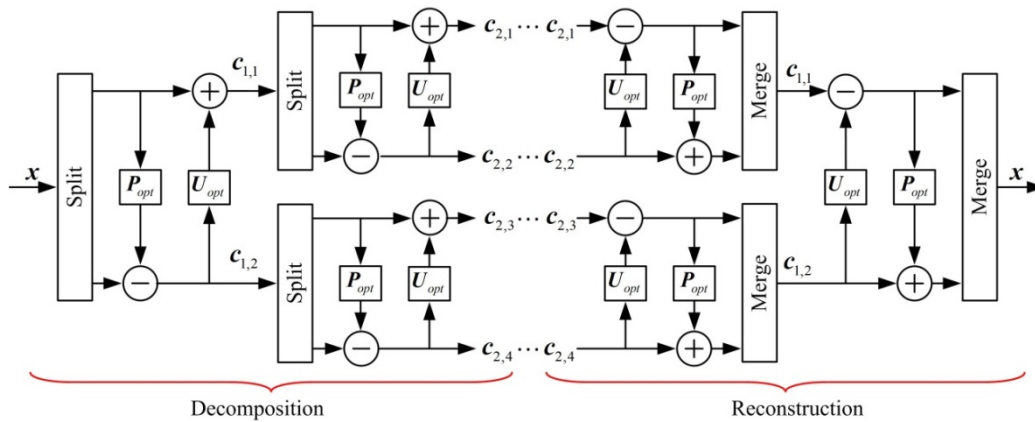

Fig. 2 The decomposition and reconstruction stages of ASGWPT

When the VSS is in different aging states, the frequency spectrum and its distribution of the vibration response signal will change. This change can be illustrated by directly observing the energy distributions of the frequency bands of ASGWPT. Moreover, the wavelet function of the developed ASGWPT can adaptively match the frequency spectrum characteristics of inspected vibration response signal, so the energy features extracted from the frequency bands of reconstructed wavelet packet coefficients possess powerful capability to reflect the different structural aging states.

After the original vibration response signal x is decomposed to level l by using ASGWPT, the 2^l frequency bands can be obtained that each frequency band has the same band width. Let $x_{l,i}$ be the reconstructed wavelet packet coefficients of the ith frequency band at level l, its energy is calculated as follows

$$E_{l,i} = \sum_{k=1}^{n} \left(x_{l,i}\left(k\right) \right)^2 \,, \qquad i = 1,2,\cdots,2^l \,, \qquad k = 1,2,\cdots,n \,, \qquad n \in Z \tag{8}$$

where n denotes the length of $x_{l,i}$. The feature vector using the extracted energy features as elements is constructed as

$$\boldsymbol{T} = \left\{ E_{l,1}, E_{l,2}, \cdots, E_{l,2^l} \right\} \tag{9}$$

Finally, for the convenience of the following analysis and processing, T is normalized as

$$\boldsymbol{T}' = \left\{ E_{l,1} / E, E_{l,2} / E, \cdots, E_{l,2^l} / E \right\} \tag{10}$$

where $E = \sum_{i=1}^{2^l} E_{l,i}$. Next, taking T' as the input vector of a classifier, the automated state classification of viscoelastic sandwich structures can be achieved.

3. Multiwavelet support vector machine and state classification

It is demonstrated in the publications (Zhang *et al*. 2004, Keskes *et al*. 2013, Liu *et al*. 2013, Chen *et al*. 2013) that SVM with the scalar wavelet kernel (WSVM) outperforms that with Gaussian kernel (SVM) in pattern recognition. As mentioned above, multiwavelets have obvious advantages compared with scalar wavelets. Motivated by this point, in order to improve the generalization ability of SVM further and obtain desired state classification result, we would like to investigate SVM with the multiwavelet kernel (MWSVM) for state classification of VSSs. As a terminal decision-making tool, the MWSVM makes use of the extracted energy features to achieve automated state classification for VSSs through state mode coding.

3.1 Summary of support vector machine

The main idea of SVM is to transform the input vectors into a higher dimensional feature space, and find the optimal separating hyper-plane that maximizes the margin between the two classes in this space by using kernel functions. Let $S = \{(x_i, y_i) \mid x_i \in R^d, y_i \in \{+1, -1\}, i = 1,..., l\}$ be a training sample set, where x_i is an input vector, d is the dimension of x_i, y_i is the label of x_i and l is the number of training samples, the decision function used by SVM to find the label of a given testing sample x is

$$f(x) = \text{sign}\left[\sum_{i=1}^{l} \alpha_i y_i K(x, x_i) + b\right] \tag{11}$$

where $K(\square)$ is the used kernel function, b is the bias value and α_i is the Lagrange multiplier obtained by solving the following dual form of quadratic optimization problem

$$\begin{cases} \max\ W(\boldsymbol{\alpha}) = \sum_{i=1}^{l} \alpha_i - \dfrac{1}{2}\sum_{i,j=1}^{l} \alpha_i \alpha_j y_i y_j K(x_i, x_j) \\[2mm] s.t.\ \ \sum_{i=1}^{l} \alpha_i y_i = 0,\ 0 \le \alpha_i \le C,\ i=1,\cdots,l \end{cases} \tag{12}$$

where C is the penalty factor implementing the trade-off between empirical risk and confidence interval.

The kernel function used in SVM can be constructed based on the Mercer's theorem. The above mentioned Gaussian kernel and scalar wavelet kernel are respectively defined as follows:

Gaussian kernel

$$K(x, x') = \exp\left(-\frac{\|x - x'\|^2}{2\sigma^2}\right) \tag{13}$$

Scalar wavelet kernel (Zhang *et al.* 2004)

$$K(x, x') = \prod_{i=1}^{d}\left(\cos\left(1.75\frac{x_i - x_i'}{a}\right)\exp\left(-\frac{\|x_i - x_i'\|^2}{2a^2}\right)\right) \tag{14}$$

where σ and a are the kernel parameters for the Gaussian and scalar wavelet kernels, respectively. Wavelet function used to construct the scalar wavelet kernel is

$$\psi(x) = \cos(1.75x)\exp\left(-\frac{x^2}{2}\right) \tag{15}$$

3.2 Summary of multiwavelets

Multiwavelets are the generalization of scalar wavelets. What the difference between them is that multiwavelet bases are generated by two or more mother wavelets. Similar to the scalar wavelet, the multiscaling functions $\Phi = [\phi_1, \phi_2,..., \phi_r]^T$ ($r > 1$) and the corresponding multiwavelet functions $\Psi = [\psi_1, \psi_2,..., \psi_r]^T$ satisfy the following two scale matrix refinement equations

$$\boldsymbol{\Phi}(t) = \sqrt{2}\sum_{k=0}^{M} \boldsymbol{H}_k \boldsymbol{\Phi}(2t - k),\quad k \in \mathbf{Z} \tag{16}$$

$$\boldsymbol{\Psi}(t) = \sqrt{2}\sum_{k=0}^{M} \boldsymbol{G}_k \boldsymbol{\Phi}(2t - k),\quad k \in \mathbf{Z} \tag{17}$$

where the coefficients $\{H_k\}$ and $\{G_k\}$ are respectively $r \times r$ matrix low-pass and high-pass filters.

In this paper, we consider a very important and widely adopted multiwavelet system named GHM multiwavelets which is constructed by Geronimo, Hardin and Massopust (Geronimo *et al.* 1994). They possess such excellent properties as orthogonality, symmetry, compact support, with approximation order 2. However, it is impossible for scalar wavelets. The two scale matrix equations of GHM multiwavelets are expressed as

$$\boldsymbol{\Phi}(t) = \begin{bmatrix} \phi_1(t) \\ \phi_2(t) \end{bmatrix} = \boldsymbol{H}_0 \boldsymbol{\Phi}(2t) + \boldsymbol{H}_1 \boldsymbol{\Phi}(2t-1) + \boldsymbol{H}_2 \boldsymbol{\Phi}(2t-2) + \boldsymbol{H}_3 \boldsymbol{\Phi}(2t-3) \tag{18}$$

where

$$\boldsymbol{H}_0 = \begin{bmatrix} \dfrac{3}{5} & \dfrac{4\sqrt{2}}{5} \\ -\dfrac{\sqrt{2}}{20} & -\dfrac{3}{10} \end{bmatrix}, \quad \boldsymbol{H}_1 = \begin{bmatrix} \dfrac{3}{5} & 0 \\ \dfrac{9\sqrt{2}}{20} & 1 \end{bmatrix}, \quad \boldsymbol{H}_2 = \begin{bmatrix} 0 & 0 \\ \dfrac{9\sqrt{2}}{20} & -\dfrac{3}{10} \end{bmatrix}, \quad \boldsymbol{H}_3 = \begin{bmatrix} 0 & 0 \\ -\dfrac{\sqrt{2}}{20} & 0 \end{bmatrix}.$$

$$\boldsymbol{\Psi}(t) = \begin{bmatrix} \psi_1(t) \\ \psi_2(t) \end{bmatrix} = \boldsymbol{G}_0 \boldsymbol{\Psi}(2t) + \boldsymbol{G}_1 \boldsymbol{\Psi}(2t-1) + \boldsymbol{G}_2 \boldsymbol{\Psi}(2t-2) + \boldsymbol{G}_3 \boldsymbol{\Psi}(2t-3) \tag{19}$$

where

$$\boldsymbol{G}_0 = \begin{bmatrix} -\dfrac{\sqrt{2}}{20} & -\dfrac{3}{10} \\ \dfrac{1}{10} & \dfrac{3\sqrt{2}}{10} \end{bmatrix}, \quad \boldsymbol{G}_1 = \begin{bmatrix} \dfrac{9\sqrt{2}}{20} & -1 \\ \dfrac{9}{10} & 0 \end{bmatrix}, \quad \boldsymbol{G}_2 = \begin{bmatrix} \dfrac{9\sqrt{2}}{20} & -\dfrac{3}{10} \\ \dfrac{9}{10} & -\dfrac{3\sqrt{2}}{10} \end{bmatrix}, \quad \boldsymbol{G}_3 = \begin{bmatrix} -\dfrac{\sqrt{2}}{20} & 0 \\ -\dfrac{1}{10} & 0 \end{bmatrix}.$$

According to Eq. (17), the two multiscaling functions $\phi_1(t)$ and $\phi_2(t)$ can be obtained. Analogously, the two mother multiwavelet functions $\psi_1(t)$ and $\psi_2(t)$ can be generated according to Eq. (18). In the following section, the two GHM multiwavelet functions $\psi_1(t)$ and $\psi_2(t)$, as shown in Fig. 3, are used to construct multiwavelet kernel functions for SVM.

3.3 Construction of multiwavelet kernel functions

Based on the two GHM multiwavelet functions, two multiwavelet kernel functions for SVM
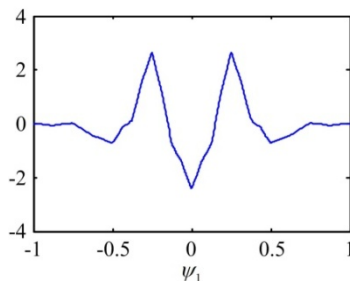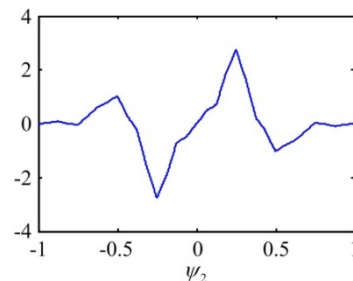
(a) Multiwavelet function 1   (b) Multiwavelet function 2

Fig. 3 The two GHM multiwavelet functions

are constructed in this section. The formation of a support vector kernel function can be expressed as either a inner product type $K(x, x') = K(\langle x \cdot x' \rangle)$ or a translation invariant type $K(x, x') = K(x - x')$. As a matter of fact, any function can serve as an admissive support vector kernel, if it satisfies the Mercer's theorem. However, it is not easy to transform a translation invariant kernel function into the product of two functions, and then to demonstrate that it is an admissive support vector kernel. For this reason, there exists the following theorem (Zhang *et al*. 2004) in place of Mercer's theorem, which provides the necessary and sufficient condition to judge whether a translation invariant kernel function can serve as an admissive support vector kernel.

Theorem 1. A translation invariant kernel function $K(x, x') = K(x - x')$ is an admissive support vector kernel, when and only when the Fourier transform of $K(x)$ satisfies the following condition

$$F[K](\omega) = (2\pi)^{-d/2} \int_{R^d} \exp(-j(\omega \cdot \boldsymbol{x})) K(\boldsymbol{x}) \mathrm{d}\boldsymbol{x} \geq 0 \tag{20}$$

Because the two GHM multiwavelet functions $\psi_1(t)$ and $\psi_2(t)$ do not satisfy the Mercer's theorem, they cannot serve as admissible support vector kernels. By the definition of the autocorrelations of the two multiwavelet functions, we have
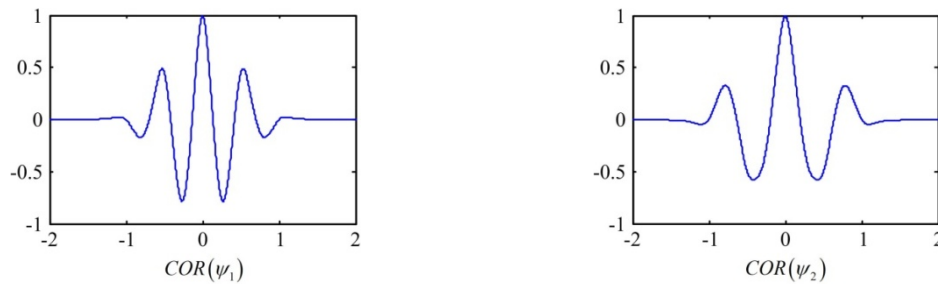
$$COR(\psi_k(t)) = \int_{-\infty}^{\infty} \psi_k(t)\psi_k(t+\tau)dt, \qquad k = 1, 2 \tag{21}$$

Based on the autocorrelations of the two multiwavelet functions, two multiwavelet kernel functions can be constructed for SVM and are defined as follows

$$K_1(\boldsymbol{x}, \boldsymbol{x}') = \prod_{i=1}^{d} COR\left(\psi_1\left(\frac{x_i - x_i'}{a}\right)\right) + \prod_{i=1}^{d} COR\left(\psi_2\left(\frac{x_i - x_i'}{a}\right)\right) \tag{22}$$

$$K_2(\boldsymbol{x}, \boldsymbol{x}') = \prod_{i=1}^{d} \left(COR\left(\psi_1\left(\frac{x_i - x_i'}{a}\right)\right) \times COR\left(\psi_2\left(\frac{x_i - x_i'}{a}\right)\right) \right) \tag{23}$$

The autocorrelations of two GHM multiwavelet functions are shown in Fig. 4. The constructed two multiwavelet kernel functions are shown in Fig. 5. These two multiwavelet kernel functions are admissible support vector kernels, and the corresponding theorem and its proof are presented as follows

(a) The autocorrelation of multiwavelet function 1   (b) The autocorrelation of multiwavelet function 2

Fig. 4 The autocorrelations of two GHM multiwavelet functions

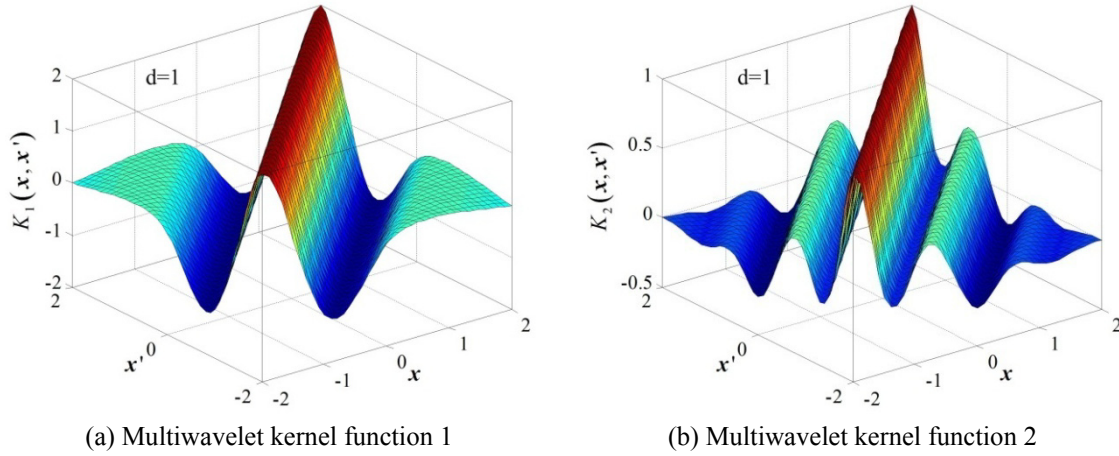(a) Multiwavelet kernel function 1   (b) Multiwavelet kernel function 2

Fig. 5 The constructed two multiwavelet kernel functions

Theorem 2. The multiwavelet kernel functions $K_1(x, x')$ and $K_2(x, x')$ constructed above are admissible support vector kernels.

Proof. It is easy to know that the Fourier transform of the autocorrelation function of $\psi_k(t)$, $k = 1, 2$, is equal to the power spectrum $|F(\psi_k)|^2$ (Chen and Dudek 2009). Due to $|F(\psi_k)|^2 \geq 0$, in accordance with the Theorem 1, we know that $COR(\psi_k((x_i - x_i')/a))$ are admissible support vector kernels. According to the construction principle of kernel functions (Shawe-Taylor and Cristianini 2004), the addition and multiplication of two admissible kernels are also admissible support vector kernels. As a result, it is obvious that the multiwavelet kernel functions $K_1(x, x')$ and $K_2(x, x')$ constructed above are admissible support vector kernels.

3.4 Multiwavelet support vector machine for state classification

The two multiwavelet kernel functions constructed above are used to develop MWSVM classifier for the state classification of VSSs, and the decision function of MWSVM is defined as

$$f(x) = \text{sign}\left[\sum_{i=1}^{l} \alpha_i y_i K_k(x, x_i) + b\right] \tag{24}$$

where $k = 1$ or 2. The selection of different k values, the different MWSVM classifiers can be obtained. Moreover, it is important to note that, in the following analysis, the MWSVM using multiwavelet kernel function 1 is denoted as MWSVM1. Similarly, the MWSVM with multiwavelet kernel function 2 is named as MWSVM2. In approximation performance, the constructed multiwavelet kernel can make up for the deficiency of scalar wavelet kernel. Thus, the built MWSVM has better classification performance than the traditional WSVM.

SVM is originally proposed for two-class classification problem, which is not applicable to state classification of VSSs, since there always appear multiple aging states in the service process of the structure. Therefore, it is necessary to develop MWSVM to deal with multi-class classification problem. Several multi-class classification strategies, such as one-against-all, one-against-one and directed acyclic graph (DAG), have been introduced by Hsu and Lin (2002), in

which they also conduct a comparison of these strategies and draw a conclusion that the one-against-one strategy is more powerful in practical applications than the other strategies. In this paper, we perform the one-against-one strategy on MWSVM for classifying the multiple aging states of VSSs.

4. The proposed aging state recognition method

In this paper, a novel method to aging state recognition of VSSs is proposed by analyzing vibration response signals, which is based on ASGWPT and multi-class MWSVM. Considering the strong non-stationarity of vibration response signals and the weakness of state change characteristics, in order to extract salient feature information to characterize the structural aging states obviously, the ASGWPT, its wavelet function can adaptively match the frequency spectrum characteristics of inspected vibration response signal, is developed to process the vibration response signals for energy feature extraction. In addition, in order to improve the generalization ability of SVM and obtain the accurate state classification result, multiwavelet kernel functions are constructed on the basis of the kernel method of SVM and multiwavelet theory, and then MWSVM is developed to accomplish the state classification of different structural aging states by using the extracted energy features. The proposed aging state recognition method for VSSs is shown in Fig. 6. It mainly includes the following several procedures.

First, when the VSS is in different aging states, by means of data acquisition system, the corresponding vibration response signals are acquired by sensors.

Second, for each of structural aging states, adaptive second generation wavelet is constructed by the design of prediction operator and update operator based on the frequency spectrum characteristics of inspected vibration response signal, and then ASGWPT is used to process the vibration response signals in the whole frequency band.

Third, energy features are extracted from the frequency bands of reconstructed wavelet packet coefficients to describe the different structural aging states.

Forth, sample data set is collected and split into a training sample set and a testing sample set.

Fifth, the training sample set is adopted to train the multi-class MWSVM classifier that is based
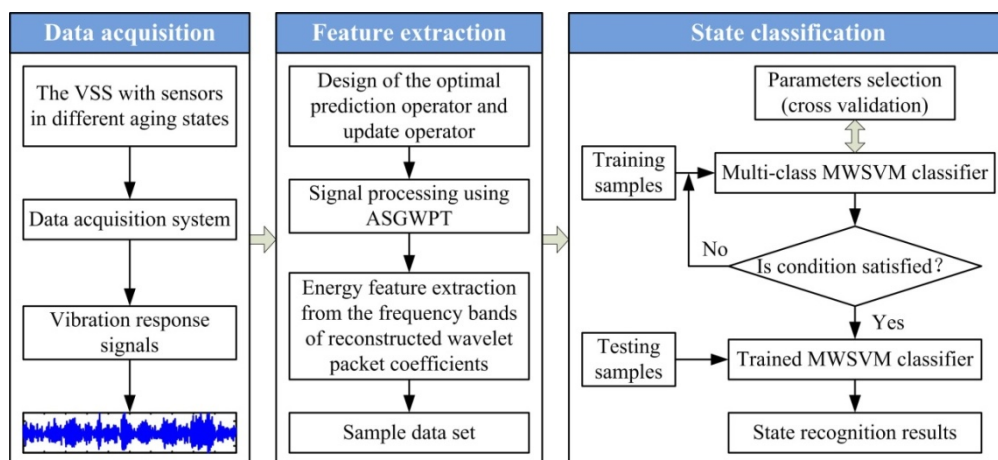

Fig. 6 The flow chart of the proposed aging state recognition method

on the one-against-one multi-class classification strategy. Herein, according to previous studies and our experimental experience, the parameters C and a of the multi-class MWSVM classifier are selected by the widely used cross validation technique in the ranges of $C = \{2^{-5}, 2^{-4}, ..., 2^{10}\}$ and $a = \{0.25, 0.5, 1.2, ..., 16\}$.

Finally, the testing sample set is fed into the trained MWSVM classifier, and then the structural aging states can be recognized according to the output of the MWSVM classifier.

It is important to note that two classifiers (MWSVM1 or MWSVM2) are respectively used in the method, the classifier which can obtain higher recognition accuracy is chosen as the final classifier.

5. Experimental results and analysis

In this section, an experiment is carried out to research the vibration response characteristics of a VSS subjected to different degrees of aging, and the corresponding vibration response signals are acquired to demonstrate the performance of the proposed aging state recognition method for VSSs.

5.1 Experimental viscoelastic sandwich structure

In order to create the different aging states of VSSs, a representative VSS is devised and manufactured, which possesses the ability to regulate the size of preload, and can conveniently change the viscoelastic layers with different aging degrees. The sketch of the experimental VSS is illustrated in Fig. 7(a), and the physical photo of the experimental VSS is shown in Fig. 7(b).

From Fig. 7, it can be seen that the experimental VSS structure is mainly constituted of steel layers with four viscoelastic layers sandwiched in. In addition, there is a connecting bolt and a force sensor. The connecting bolt is adopted to impose a preload on the structure to compress the steel layers and viscoelastic layers, and the force sensor is employed to measure the size of
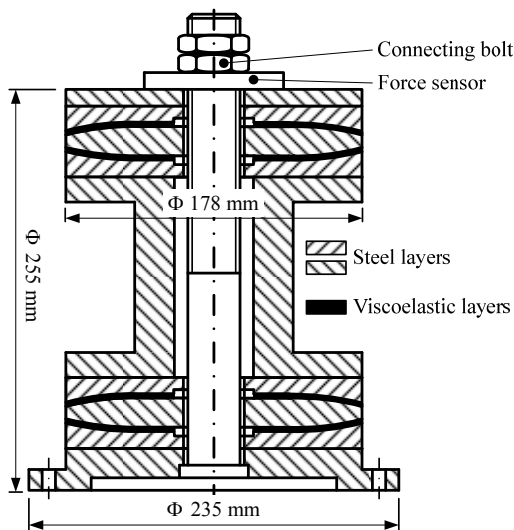
(a) The sketch of the structure 　　　　　(b) The physical photo of the structure

Fig. 7 The sketch and the physical photo of the experimental VSS

preload. Then, a certain size of preload can be imposed on the structure by adjusting the connecting bolt and monitoring the force sensor. In this study, rubber material is chosen as the viscoelastic material and tailored to the needed viscoelastic layers.

5.2 Hot oxygen accelerated aging of viscoelastic material

In the practical engineering application, structural aging is a time-consuming process, and the aging of VSSs is mainly resulted from the aging of viscoelastic material. Therefore, in this paper, in order to create the different aging states of the experimental VSS, the hot oxygen accelerated aging of viscoelastic material is carried out. On the basis of the research conclusions presented in the publication (Woo *et al*. 2010), some of the rubber material specimens are input into an environmental chamber for hot oxygen accelerated aging.

As shown in Fig. 8, the environmental chamber has such functions as temperature regulation, continuous air blast, air intake and exhaust. By controlling the environmental conditions of environmental chamber and the duration of aging, the viscoelastic material can achieve a certain degree of accelerated aging. In this study, the temperature of environmental chamber is set to 110°C, and the way of air circulation is chosen as forced air blast. Moreover, the duration of aging is used to describe the aging degree of viscoelastic material.

As shown in Fig. 9, the placement of rubber material specimens in environmental chamber is in a hanging and hierarchical manner. Furthermore, in order to ensure that the hot air of environmental chamber is circulated, the aging degree of rubber material is uniform and the phenomenon two adjacent specimens sticking together is averted, the distance between two neighboring specimens is at least 10 mm, and the distance between the specimen and the wall to be not less than 70 mm. There are three kinds of rubber material specimens. The specimens A are the viscoelastic layers those are employed to sandwich in the experimental VSS. The specimens B and C are adopted to implement the compressive property tests and tensile property tests of the rubber material with different aging degrees, respectively.

According to the sampling plan, when the predetermined aging duration comes, a set of rubber material specimens which include four viscoelastic layers, three tensile specimens and one
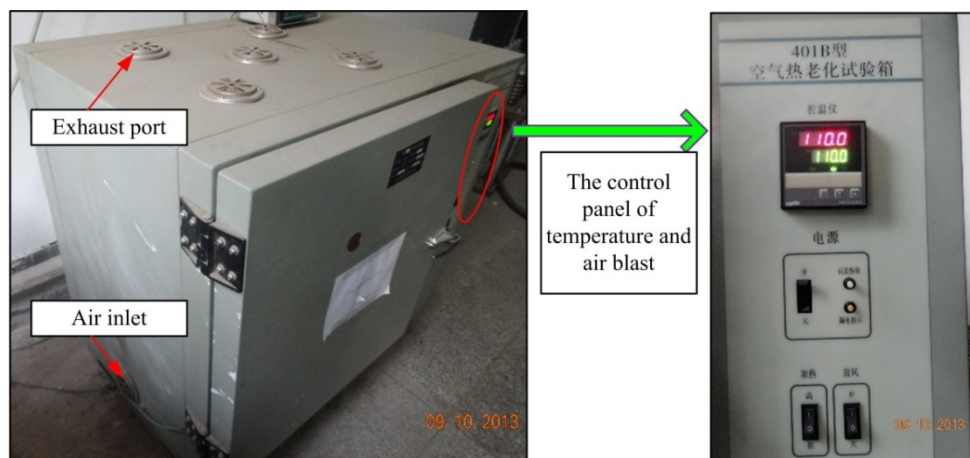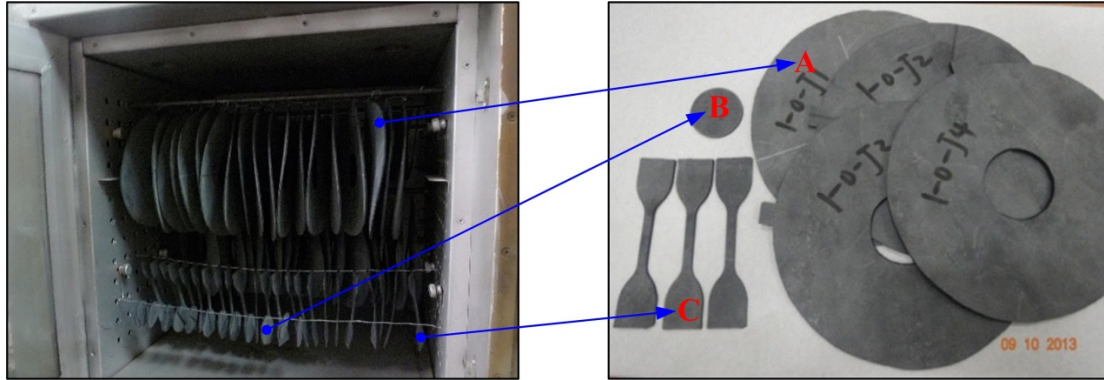

Fig. 8 Environmental chamber

Fig. 9 The aging specimens

compressive specimen are taken out and regarded as an aging state. In this way, we finally obtain thirteen sets of rubber material specimens which correspond to thirteen aging states. The corresponding aging days of the thirteen aging states, respectively, are 0, 1, 3, 5, 7, 9, 11, 14, 17, 20, 23, 26 and 29.

In order to characterize the aging phenomena of the rubber material in thirteen aging states, according to the national standard of China (GB/T 7757-2009), the compressive property tests of the thirteen sets of compressive specimens in different aging states are carried out. For each aging state, the big compressive specimen is tailored to three small specimens with diameter of 10mm, and the test result is the average of three small compressive specimens. The amount of compression and compression rate are set as 1 mm and 0.5 mm/min, respectively. The corresponding compressive stress-strain curve and elasticity modulus are shown in Fig. 10(a) and Fig. 10(b), respectively. Moreover, according to the national standard of China (GB/T 528-2009), the tensile property tests of the thirteen sets of tensile specimens in different aging states are also performed. For each aging state, the test result is the average of these tensile specimens which are snapped normally. The compression rate is set as 100 mm/min, and the corresponding tensile stress-strain curve and elasticity modulus are shown in Figs. 11(a) and (b), respectively.
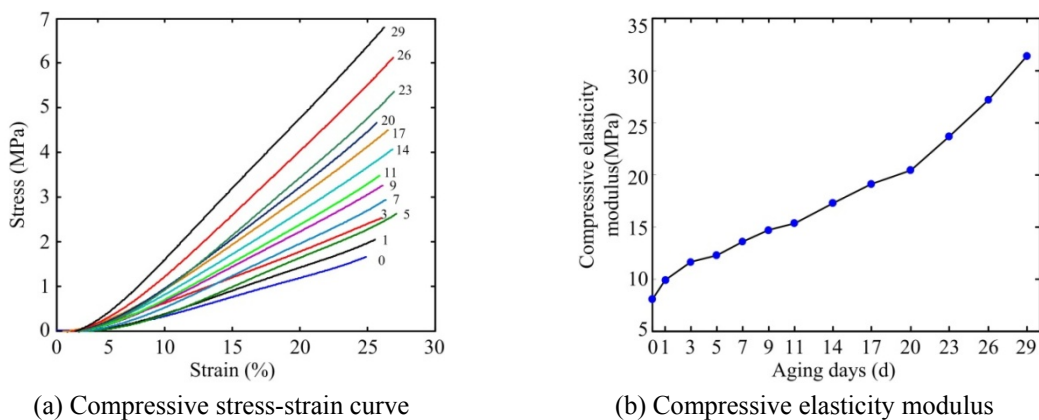

(a) Compressive stress-strain curve

(b) Compressive elasticity modulus

Fig. 10 The results of compressive property tests

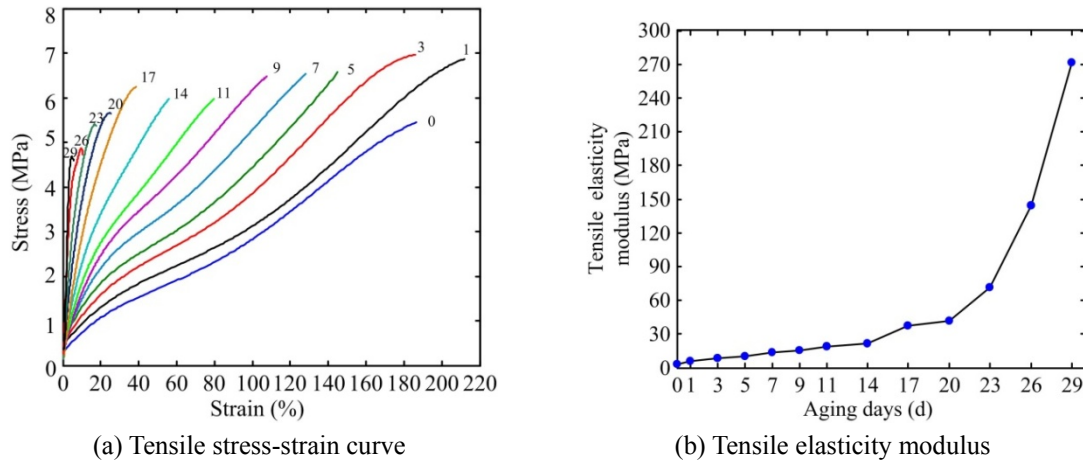(a) Tensile stress-strain curve   (b) Tensile elasticity modulus

Fig. 11 The results of tensile property tests

From Figs. 10(a) and 11(a), we can see that, when the compressive stress and the tensile stress are in a certain value, the compressive strain and tensile strain of rubber material gradually become smaller with the increment of aging days. From Figs. 10(b) and 11(b), it can be seen that, along with the increment of aging days, the compressive elasticity modulus and tensile elasticity modulus of rubber material gradually increase. All the above analysis results show that, the aging degrees of the rubber material in thirteen aging states are gradually deepening with aging days increasing.

5.3 Experiment setup and data acquisition

When a certain size of preload is imposed on the experimental VSS, thirteen structural aging states can be created by replacing the viscoelastic layers with the thirteen aging degrees. According to the results of compressive property tests, the size of the preload imposed on the structure is intended to be 7500 N. That is because the viscoelastic layers sandwiched in the experimental VSS mainly endure compressive stress. In addition, under the action of this preload, the compressive elasticity modulus of the rubber material in thirteen aging states changes significantly. The aging days of the viscoelastic layers for each structural aging state is shown in Table 1, and the thirteen structural aging states are denoted by AS1-AS13, respectively. Corresponding to the thirteen aging states of the viscoelastic material, the aging degrees in the thirteen structural aging states are also gradually deepening.

In order to acquire the vibration response signals of the experimental VSS in different aging states, an experimental system, as shown in Fig. 12(a), is built for random excitation. We can see from Fig. 12(a) that, the experimental system primarily consists of the experimental VSS

Table 1 The aging state description of the experimental VSS

	Aging state and label												
	AS1	AS2	AS3	AS4	AS5	AS6	AS7	AS8	AS9	AS10	AS11	AS12	AS13
Aging days	0	1	3	5	7	9	11	14	17	20	23	26	29

with acceleration sensors, a force display instrument, a data acquisition system, a vibration table and the corresponding vibration table control system. The arrangement of acceleration sensors is shown in Fig. 12(b). It can be seen from Fig. 12(b) that, twelve acceleration sensors are mounted on the surface of the structure, six of them are used to measure the vibration response signals from axial direction, and the other six are used to measure the vibration response signals from radial direction. In addition, the angle between two sensors in the same horizontal plane is probably 120 degrees. By means of the force sensor, the force display instrument is used to display the size of the preload imposed on the structure. The experimental VSS in each of aging states is installed on the vibration table and randomly excited in vertical direction. The random excitation signal, applied to the structure via the vibration table, is generated through the vibration table control system. Moreover, the power spectrum density (PSD) of the random excitation signal in the frequency range of 10-2000 Hz is shown in Fig. 13. Under the above described random excitation, the vibration response signals of the experimental VSS in all aging states are measured through the twelve acceleration sensors and then stored by the data acquisition system. Moreover, when data acquisition is implemented, the sampling frequency and the sampling time of each aging state are set to10240 Hz and 120 seconds, respectively.

(a) Experimental system   (b) The arrangement of twelve acceleration sensors
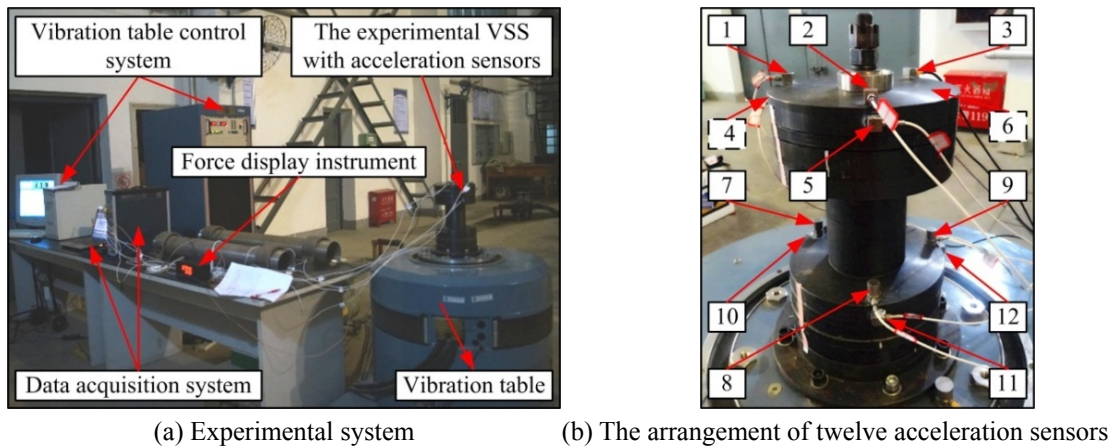
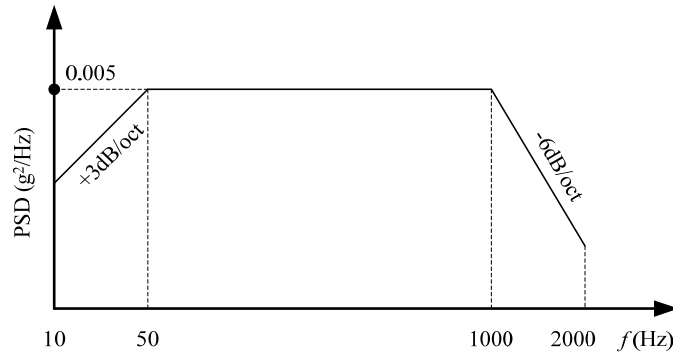Fig. 12 Experimental system and sensor arrangement

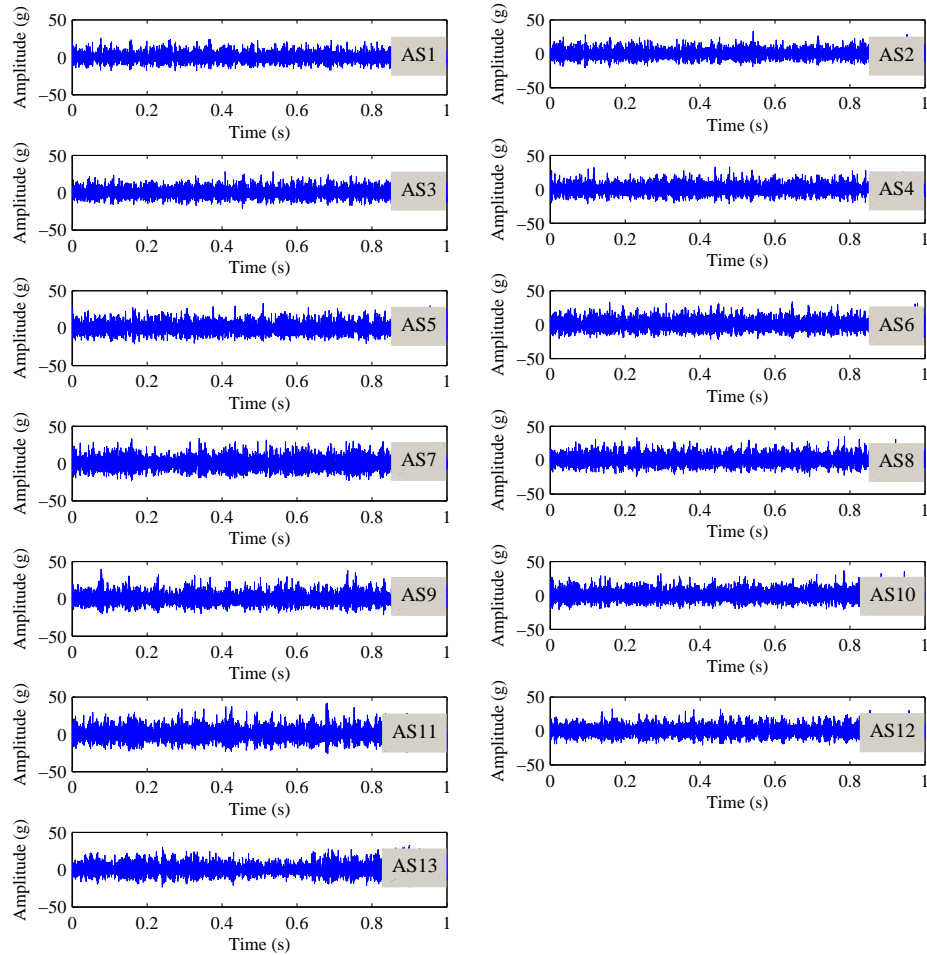Fig. 13 The power spectrum density (PSD) of random excitation signal

Fig. 14 The vibration response signals of the thirteen structural aging states

It should be noted especially that the proposed method only needs the vibration response signals from one sensor. Furthermore, since the direction of random excitation is vertical, the axial vibration response signals contain the main vibration response information of the experimental VSS. Therefore, after data acquisition, the vibration response signals measured by sensor 1 are adopted to demonstrate the effectiveness of the proposed method in recognizing the different aging states of the experimental VSS.

The vibration response signals of the thirteen structural aging states are displayed in Fig. 14. It can be seen in Fig. 14 that, only using the vibration response signals, it is not easy to recognize the thirteen aging states of the experimental VSS. Thus, in order to recognize the thirteen different aging states of the experimental VSS accurately, it is very essential to develop an effective method to extract the state features which are sensitive to the different aging state.

5.4 Performance analysis of the proposed method

On the basis of the above experiment, the data set containing the vibration response signals of

the thirteen aging states of the experimental VSS is collected to evaluate the performance of the proposed aging state recognition method. When performing the proposed method, the vibration response signal of each aging state is divided into 60 non-overlapping samples with each sample consisting of 2048 data points. The 60 samples of each aging state are split into 30 for training and the other 30 for testing.

First of all, in order to extract sensitive feature information to the different structural aging state from the complex vibration response signals, one sample of each aging state is taken out and regarded as the representative vibration response signal to construct adaptive second generation wavelet by the design of prediction operator and update operator. The numbers of prediction coefficients and update coefficients are all chosen as 6. On the basis of the optimization design methods of prediction operator and update operator mentioned in Section 2.2, the optimal prediction operators and update operators of the thirteen structural aging states are obtained, which can adaptively match the frequency spectrum characteristics of the corresponding vibration response signals. The designed optimal prediction operators and update operators corresponding to the thirteen structural aging states are displayed in Table 2, respectively.

After that, all of the vibration response signals are processed by using the developed ASGWPT with level 3, and then eight energy features are extracted from the frequency bands of reconstructed wavelet packet coefficients to reveal the different aging states of the experimental VSS. For the each of structural aging states, taking one sample as instance, the energy distributions of the frequency bands of ASGWPT are shown in Fig. 15. We can find from Fig. 15 that, when the experimental VSS is in different aging states, the corresponding energy distributions of the frequency bands of ASGWPT are obvious different from each other and can separate the various aging states to a certain degree. That is to say, the eight energy features extracted on the basis of ASGWPT are effective to recognize the different aging states of the experimental VSS. Nevertheless, supposing that the different structural aging states are recognized by the operator according to the extracted eight energy features, the tedious recognition process and inaccurate recognition result are difficult to be accepted. Therefore, an intelligent technique is needed to implement the accurate and automated recognition of the different structural aging states.

Table 2 The optimal prediction operators and update operators of the thirteen structural aging states

| State	Prediction operator	Update operator
AS1	[0.4699, -0.3854, 0.4155, 0.4155, -0.3854, 0.4699]	[0.0999, -0.0613, 0.2115, 0.2115, -0.0613, 0.0999]
AS2	[0.5193, -0.3785, 0.3592, 0.3592, -0.3785, 0.5193]	[0.0659, -0.0705, 0.2546, 0.2546, -0.0705, 0.0659]
AS3	[0.2479, -0.2649, 0.5170, 0.5170, -0.2649, 0.2479]	[0.2415, -0.0573, 0.0658, 0.0658, -0.0573, 0.2415]
AS4	[0.1804, -0.5708, 0.8905, 0.8905, -0.5708, 0.1804]	[0.0785, -0.0630, 0.2344, 0.2344, -0.0630, 0.0785]
AS5	[0.2008, -0.1688, 0.4680, 0.4680, -0.1688, 0.2008]	[0.2445, -0.0687, 0.0742, 0.0742, -0.0687, 0.2445]
AS6	[0.4154, -0.3303, 0.4148, 0.4148, -0.3303, 0.4154]	[0.1267, -0.0738, 0.1972, 0.1972, -0.0738, 0.1267]
AS7	[0.1106, -0.4165, 0.8060, 0.8060, -0.4165, 0.1106]	[0.1617, -0.0755, 0.1638, 0.1638, -0.0755, 0.1617]
AS8	[0.1268, -0.3322, 0.7054, 0.7054, -0.3322, 0.1268]	[0.1652, -0.0878, 0.1726, 0.1726, -0.0878, 0.1652]
AS9	[0.0847, -0.2815, 0.6968, 0.6968, -0.2815, 0.0847]	[0.2489, -0.0925, 0.0936, 0.0936, -0.0925, 0.2489]
AS10	[-0.3031, 0.0387, 0.7644, 0.7644, 0.0387, -0.3031]	[0.3492, -0.0500, -0.0491, -0.0491, -0.0500, 0.3492]
AS11	[-0.2353, -0.0156, 0.7509, 0.7509, -0.0156, -0.2353]	[0.3578, -0.0468, -0.0610, -0.0610, -0.0468, 0.3578]
AS12	[-0.1186, -0.1019, 0.7204, 0.7204, -0.1019, -0.1186]	[0.3240, -0.0242, -0.0498, -0.0498, -0.0242, 0.3240]
AS13	[-0.6740, 0.2340, 0.9400, 0.9400, 0.2340, -0.6740]	[0.3307, -0.0711, -0.0096, -0.0096, -0.0711, 0.3307]
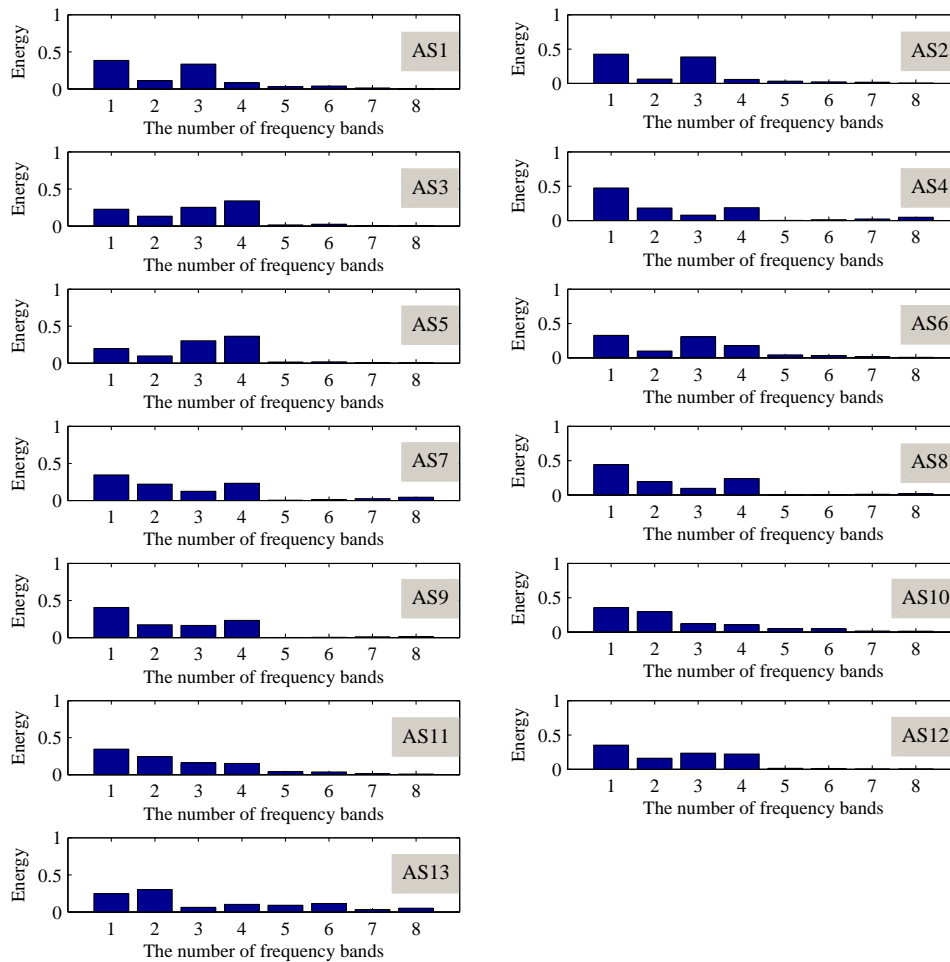
Fig. 15 The energy distributions of the frequency bands of ASGWPT for thirteen aging states

Finally, the developed MWSVM is applied to achieve the accurate and automated aging state recognition of the experimental VSS. Using the extracted eight energy features as the input features, the multi-class MWSVM classifier is respectively trained and tested to classify the thirteen structural aging states. The testing results are presented in Table 3.

It can be seen from the testing results in Table 3 that, in the case of MWSVM1, the recognition accuracy of AS5 is 93.33% (there are only 2 incorrectly recognized testing samples), the recognition accuracies of the other aging states are all 100% (for each of these aging states, there no incorrectly recognized testing samples), and the average recognition accuracy reaches to 99.49%. In the case of MWSVM2, the recognition accuracies of AS3 and AS5 are all 96.67% (for each of the two aging states, there is only 1 incorrectly recognized testing samples), the recognition accuracies of the other aging states are all 100% (for each of these aging states, there no incorrectly recognized testing samples), and the average recognition accuracy as well reaches to 99.49%. All the above analysis results show that the proposed method can accurately and automatically recognize the different aging states of the experimental VSS, and can act as a promising approach to aging state recognition of VSSs.

Table 3 The performance analysis of the proposed method

State	MWSVM1 ($C = 2^8$, $a = 4$)		MWSVM2 ($C = 2^9$, $a = 4$)	
	Recognized number[*]	Recognition accuracy[*] (%)	Recognized number	Recognition accuracy (%)
AS1	30 (30+0)	100	30 (30+0)	100
AS2	30 (30+0)	100	30 (30+0)	100
AS3	32 (30+2)	100	30 (29+1)	96.67
AS4	30 (30+0)	100	30 (30+0)	100
AS5	28 (28+0)	93.33	30 (29+1)	96.67
AS6	30 (30+0)	100	30 (30+0)	100
AS7	30 (30+0)	100	30 (30+0)	100
AS8	30 (30+0)	100	30 (30+0)	100
AS9	30 (30+0)	100	30 (30+0)	100
AS10	30 (30+0)	100	30 (30+0)	100
AS11	30 (30+0)	100	30 (30+0)	100
AS12	30 (30+0)	100	30 (30+0)	100
AS13	30 (30+0)	100	30 (30+0)	100
Average		99.49		99.49

* Recognized number includes two parts: the former is the correctly recognized testing sample number and the latter is the incorrectly recognized number
* Recognition accuracy is defined as the percentage of the correctly recognized testing sample number from the total

5.5 Performance comparison analysis of the proposed method

5.5.1 Comparison of ASGWPT with SGWPT for feature extraction

In order to validate the superiority of ASGWPT in processing the strong non-stationary vibration response signals for feature extraction, the commonly used SGWPT is applied for comparison. For SGWPT, the decomposition level, the number of prediction coefficients and the number of update coefficients are all same with ASGWPT. The difference is that, the prediction and update operators of SGWPT are irrelevant to the vibration response signals, and are gained through the equivalent filter method presented in the publication (Claypoole *et al*. 2003). The same vibration response signals are processed by using SGWPT, and eight energy features are extracted from the frequency bands of reconstructed wavelet packet coefficients to reflect the different structural aging states. For the thirteen structural aging states, with one sample, for example, the energy distributions of the frequency bands of SGWPT are shown in Fig. 16. It can be seen from Fig. 16 that, when the experimental VSS is in different aging states, the energy distributions of the frequency bands of SGWPT are basically the same. In other words, on the basis of the energy features extracted by using SGWPT, it is difficult to accurately recognize the thirteen aging states of the experimental VSS. Furthermore, taking these features as the input features, the multi-class MWSVM classifier is respectively trained and tested to classify the thirteen structural aging states. The testing results are listed in Table 4.

Examining the testing results in Table 4, a number of things can be seen. First, for MWSVM1, taking the energy features extracted by using SGWPT as the input features, there are a total of 188
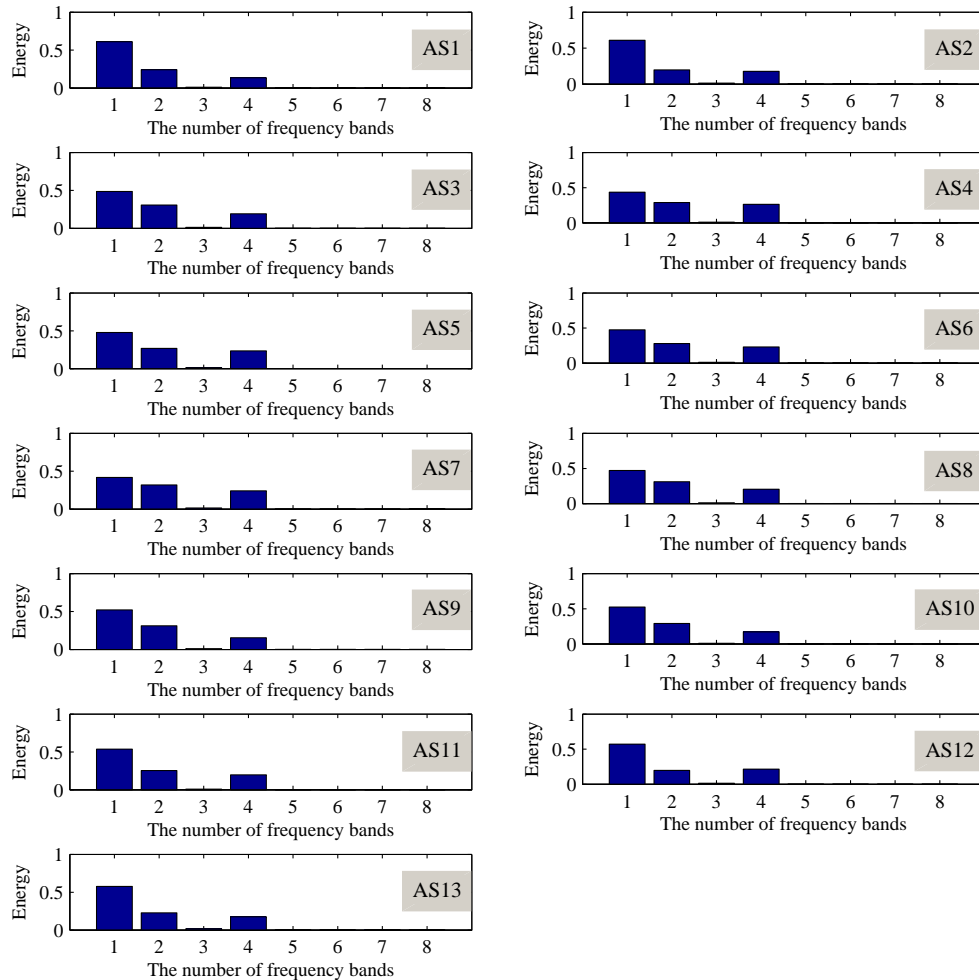
Fig. 16 The energy distributions of the frequency bands of SGWPT for thirteen aging states

incorrectly recognized testing samples and the average recognition accuracy is 51.79%. Moreover, for MWSVM2, taking the energy features extracted by using SGWPT as the input features, there are a total of 190 incorrectly recognized testing samples and the average recognition accuracy is 51.28%. Compared with those taking the energy features extracted by using ASGWPT as the input features, the MWSVM1 classifier decreases the average recognition accuracy by 47.7%, and the MWSVM2 classifier decreases the average recognition accuracy by 48.21%.

Based on all the above analysis and comparison results, it can be validated that, since the wavelet function of ASGWPT can adaptively match the frequency spectrum characteristics of the inspected vibration response signal, the developed ASGWPT is a more effective method in processing the complex vibration response signals for feature extraction than the traditional SGWPT, and hence the extracted energy features by using ASGWPT are more powerful in recognizing the different aging states of the experimental VSS than those by using SGWPT.

Moreover, the energy entropy is analyzed to further validate effectiveness of ASGWPT for structural health monitoring. The energy entropy using ASGWPT of every sample for thirteen
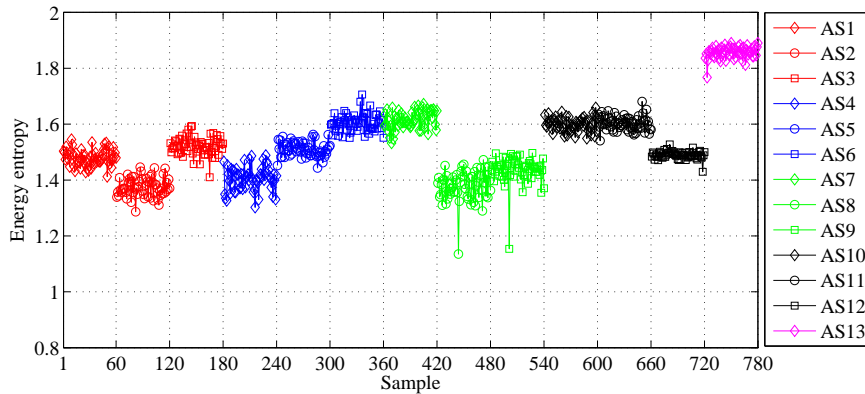
Fig. 17 The energy entropy using ASGWPT of every sample for thirteen aging states
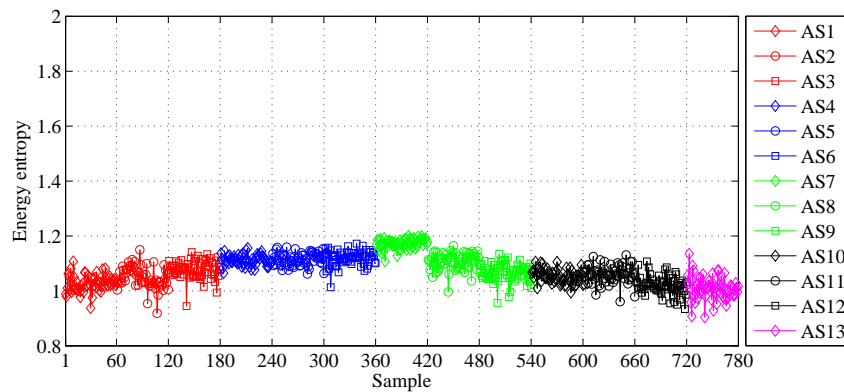

Fig. 18 The energy entropy using SGWPT of every sample for thirteen aging states

aging states is shown in Fig. 17, and the energy entropy using SGWPT of every sample for thirteen aging states is shown in Fig. 18.

By comparing Figs. 17 and 18, it can be seen that, the energy entropy using ASGWPT can better separate the thirteen structural aging states than the energy entropy using SGWPT. It also demonstrates that ASGWPT is more effectiveness than SGWPT for structural health monitoring.

5.5.2 Comparison of MWSVM with WSVM for state classification

In order to validate the performance of MWSVM in classifying the different aging states of VSSs, the recently developed WSVM is chosen as reference. As with MWSVM, the adopted multi-class classification strategy of WSVM is also one-against-one, and the parameters C and a of WSVM are also selected by using the cross validation method in the same ranges. Taking the eight energy features extracted by using ASGWPT as the input features, the multi-class WSVM classifier is respectively trained and tested to classify the thirteen aging states of the experimental VSS. The testing results are displayed in Table 4.

Observing the testing results in Table 4, it can be seen that, taking the energy features extracted by using ASGWPT as the input features of the WSVM classifier, there are a total of 27 incorrectly recognized testing samples and the corresponding average recognition accuracy is 93.08%. By

Table 4 The performance comparison analysis of the proposed method

State	The method using SGWPT for feature extraction				The method using WSVM for state classification	
	MWSVM1 ($C = 2^7$, $a = 1$)		MWSVM2 ($C = 2^7$, $a = 1$)		($C = 2^6$, $a = 2$)	
	Recognized number	Recognition accuracy (%)	Recognized number	Recognition accuracy (%)	Recognized number	Recognition accuracy (%)
AS1	41 (17+24)	56.67	41 (14+27)	46.67	31 (29+2)	96.67
AS2	32 (13+19)	43.33	34 (13+21)	43.33	29 (28+1)	93.33
AS3	35 (13+22)	43.33	32 (12+20)	40	24 (16+8)	53.33
AS4	28 (15+13)	50	31 (17+14)	56.67	30 (30+0)	100
AS5	34 (16+18)	53.33	35 (16+19)	53.33	36 (22+14)	73.33
AS6	30 (14+16)	46.67	27 (14+13)	46.67	29 (29+0)	96.67
AS7	34 (30+4)	100	34 (30+4)	100	30 (30+0)	100
AS8	20 (12+8)	40	18 (11+7)	36.67	30 (30+0)	100
AS9	14 (8+6)	26.67	17 (9+8)	30	30 (30+0)	100
AS10	39 (20+19)	66.67	41 (22+19)	73.33	30 (30+0)	100
AS11	26 (12+14)	40	24 (11+13)	36.67	32 (30+2)	100
AS12	22 (10+12)	33.33	21 (9+12)	30	29 (29+0)	96.67
AS13	35 (22+13)	73.33	35 (22+13)	73.33	30 (30+0)	100
Average		51.79		51.28		93.08

*Notations are the same as those used in Table 3

using the extracted energy features based on ASGWPT as the input features, MWSVM1 and MWSVM2 all improve the average recognition accuracy by 6.41% than WSVM.

All the above analysis and comparison results validate that, since multiwavelets possess many good properties that scalar wavelets do not have, the constructed multiwavelet kernel functions by using multiwavelet functions can make the developed MWSVM to possess better performance in classify the different aging states of VSSs, and hence MWSVM can achieve higher recognition accuracy than WSVM in classifying the different aging states of the experimental VSS.

6. Conclusions

By the analysis of vibration response signals, a novel method for aging state recognition of viscoelastic sandwich structures (VSSs) is proposed in this paper, which is based on adaptive second generation wavelet packet transform (ASGWPT) and multiwavelet support vector machine (MWSVM). In order to derive sensitive feature information to different structural aging states from the strong non-stationary vibration response signals, the adaptive second generation wavelet which can adaptively match the frequency spectrum characteristics of inspected vibration response signal is constructed, and then the ASGWPT is developed to process the vibration response signals in the whole frequency band and energy features are extracted from the frequency bands of reconstructed wavelet packet coefficients to describe the different structural aging states. Moreover, in order to improve the generalization ability of SVM and obtain the desired state classification

result, based on the kernel method of SVM and multiwavelet theory, multiwavelet kernel functions are constructed for SVM, and then the MWSVM is developed for classifying the various structural aging states by using the extracted energy features.

In order to validate the effectiveness of the proposed aging state recognition method, different aging states of the experimental VSS are created through the hot oxygen accelerated aging of viscoelastic material. The random excitations of the structure in all aging states are carried out and the corresponding vibration response signals are measured to be analyzed. The application results indicate that, profited from the combination of ASGWPT for feature extraction and MWSVM for state classification, the proposed method can recognize the different structural aging states accurately and automatically, and can hold significant promise in aging state recognition of VSSs. In addition, the developed ASGWPT is more powerful in processing the complex vibration response signals for feature extraction than the commonly used SGWPT, and the developed MWSVM possesses better performance in classify the different structural aging states compared with the recently sprung up WSVM.

The engineering application of the proposed method is part of future work. Furthermore, in engineering practice, the aging of VSSs often occurs along with looseness, these two kinds of damage may add together and interfere with each other. This situation will make state recognition of VSSs more complicated and difficult. Therefore, the effective method for this task needs to be explored in future work.

Acknowledgments

References

Bilasse, M., Azrar, L. and Daya, E.M. (2011), "Complex modes based numerical analysis of viscoelastic sandwich plates vibrations", *Comput. Struct.*, **89**(7), 539-555.

Carden, E.P. and Fanning, P. (2004), "Vibration based condition monitoring: a review", *Struct. Health Monitor.*, **3**(4), 355-377.

Chen, G.Y. and Dudek, G. (2009), "Auto-correlation wavelet support vector machine", *Image Vision Comput.*, **27**(8), 1040-1046.

Chen, F.F., Tang, B.P. and Chen, R.X. (2013), "A novel fault diagnosis model for gearbox based on wavelet support vector machine with immune genetic algorithm", *Measurement*, **46**(1), 220-232.

Chen, J.L., Zhang, C.L., Zhang, X.Y., Zi, Y.Y., He, S.L. and Yang, Z. (2015), "Planetary gearbox condition monitoring of ship-based satellite communication antennas using ensemble multiwavelet analysis method", *Mech. Syst. Signal Process.*, **54**, 277-292.

Claypoole, R.L., Davis, G.M., Sweldens, W. and Baraniuk, R. (2003), "Nonlinear wavelet transforms for image coding via lifting", *IEEE Trans. Image Process.*, **12**(12), 1449-1459.

Daubechies, I. (1992), *Ten Lectures on Wavelets*, SIMA, Philadelphia, PA, USA.

Fan, W. and Qiao, P.Z. (2011), "Vibration-based damage identification methods: a review and comparative study", *Struct. Health Monitor.*, **10**(1), 83-111.

Geronimo, J.S., Hardin, D.P. and Massopust, P.R. (1994), "Fractal functions and wavelet expansions based on several scaling functions", *J. Approx. Theory*, **78**(3), 373-401.

Gouze, A., Antonini, M., Barlaud, M. and Macq, B. (2004), "Design of signal-adapted multidimensional lifting scheme for lossy coding", *IEEE Trans. Image Process.*, **13**(12), 1589-1603.

Hou, Z.M., Xia, H. and Zhang, Y.L. (2012), "Dynamic analysis and shear connector damage identification of steel-concrete composite beams", *Steel Compos. Struct.*, *Int. J.*, **13**(4), 327-341.

Hsu, C.W. and Lin, C.J. (2002), "A comparison of methods for multiclass support vector machines", *IEEE Trans. Neural Networks.*, **13**(2), 415-425.

Hu, Q., He, Z.J., Zhang, Z.S. and Zi, Y.Y. (2007), "Fault diagnosis of rotating machinery based on improved wavelet package transform and SVMs ensemble", *Mech. Syst. Signal Process.*, **21**(2), 688-705.

Kapur, J.H. and Kesavan, H.K. (1992), *Entropy Optimization Principles with Application*, Academic Press, New York, NY, USA.

Keskes, H., Braham, A. and Lachiri, Z. (2013), "Broken rotor bar diagnosis in induction machines through stationary wavelet packet transform and multiclass wavelet SVM", *Elec. Power Syst. Res.*, **97**, 151-157.

Leng, J.F., Chen, D.H. and Jing, S.X. (2007), "Mine fan intelligent faults diagnosis based on the lifting wavelet packet and RBF neuralnet work", *Proceedings of the Fourth International Conference on Fuzzy Systems and Knowledge Discovery*, Haikou, China, August.

Li, Z., He, Z.J., Zi, Y.Y. and Jiang, H.K. (2008), "Rotating machinery fault diagnosis using signal-adapted lifting scheme", *Mech. Syst. Signal Process.*, **22**(3), 542-556.

Liu, Z.W., Cao, H.R., Chen, X.F., He, Z.J. and Shen, Z.J. (2013), "Multi-fault classification based on wavelet SVM with PSO algorithm to analyze vibration signals from rolling element bearings", *Neurocomputing*, **99**, 399-410.

Meng, L.J., Xiang, J.W., Wang, Y.X., Jiang, Y.Y. and Gao, H.F. (2015a), "A hybrid fault diagnosis method using morphological filter–translation invariant wavelet and improved ensemble empirical mode decomposition", *Mech. Syst. Signal Process.*, **50-51**, 101-115.

Meng, L.J., Xiang, J.W., Zhong, Y.T. and Song, W.L. (2015b), "Fault diagnosis of rolling bearing based on second generation wavelet denoising and morphological filter", *J. Mech. Sci. Technol.*, **29**(8), 3121-3129.

Moita, J.S., Araújo, A.L., Martins, P., Mota Soares, C.M. and Mota Soares, C.A. (2011), "Finite element model for damping optimization of viscoelastic sandwich structures", *Comput. Struct.*, **89**(21), 1874-1881.

Pan, Y.N., Chen, J. and Guo, L. (2009), "Robust bearing performance degradation assessment method based on improved wavelet packet-support vector data description", *Mech. Syst. Signal Process.*, **23**(3), 669-681.

Peng, Z.K. and Chu, F.L. (2004), "Application of the wavelet transform in machine condition monitoring and fault diagnostics: a review with bibliography", *Mech. Syst. Signal Process.*, **18**(2), 199-221.

Qu, J.X., Zhang, Z.S., Wen, J.P., Guo, T., Luo, X., Sun, C. and Li, B. (2014), "State recognition of the viscoelastic sandwich structure based on adaptive redundant second generation wavelet packet transform, permutation entropy and wavelet support vector machine", *Smart Mater. Struct.*, **23**(8) 085004.

Shawe-Taylor, J. and Cristianini, N. (2004), *Kernel Methods for Pattern Analysis*, Cambridge University Press, Cambridge, MA, USA.

Si, Y., Zhang, Z.S., Cheng, W. and Yuan, F.C. (2015), "State detection of explosive welding structure by dual-tree complex wavelet transform based permutation entropy", *Steel Compos. Struct.*, *Int. J.*, **19**(3), 569-583.

Sun, C., Zhang, Z.S., Guo, T., Luo, X., Qu, J.X. and Li, B. (2014a), "A novel manifold-manifold distance with its application to looseness state assessment of viscoelastic sandwich structure", *Smart Mater. Struct.*, **23**(6) 065019.

Sun, H.L., He, Z.J., Zi, Y.Y., Yuan, J., Wang, X.D., Chen, J.L. and He, S.L. (2014b), "Multiwavelet transform and its applications in mechanical fault diagnosis-A review", *Mech. Syst. Signal Process.*, **43**(1), 1-24.

Sweldens, W. (1998), "The lifting scheme: a construction of second generation wavelets", *SIAM J. Math. Anal.*, **29**(2), 511-546.

Vapnik, V.N. (2000), *The Nature of Statistical Learning Theory*, Springer, New York, NY, USA.

Woo, C.S., Choi, S.S., Lee, S.B. and Kim, H.S. (2010), "Useful lifetime prediction of rubber components using accelerated testing", *IEEE Trans. Reliab.*, **59**(1), 11-17.

Xiang, J.W., Matsumoto, T., Long, J.Q., Wang, Y.X. and Jiang, Z.S. (2012), "A simple method to detect cracks in beam-like structures", *Smart Struct. Syst.*, *Int. J.*, **9**(4), 335-353.

Xiang, J.W., Nackenhorst, U., Wang, Y.X., Jiang, Y.Y., Gao, H.F. and He, Y.M. (2014), "A new method to

detect cracks in plate-like structures with though-thickness cracks", *Smart Struct. Syst., Int. J.*, **14**(3), 397-418.

Xiang, J.W., Zhong, Y.T. and Gao, H.F. (2015), "Rolling element bearing fault detection using PPCA and spectral kurtosis", *Measurement*, **75**, 180-191.

Yan, Y.J., Cheng, L., Wu, Z.Y. and Yam, L.H. (2007), "Development in vibration-based structural damage detection technique", *Mech. Syst. Signal Process.*, **21**(5), 2198-2211.

Yan, R.Q., Gao, R.X. and Chen, X.F. (2014), "Wavelets for fault diagnosis of rotary machines: a review with applications", *Signal Process.*, **96**(Part A), 1-15.

Zhang, X.W., Gao, R.X., Yan, R.Q, Chen, X.F., Sun, C. and Yang, Z.B. (2016), "Multivariable wavelet finite element-based vibration model for quantitative crack identification by using particle swarm optimization", *J. Sound Vib.*, **375**, 200-216.

Zhang, L., Zhou, W.D. and Jiao, L.C. (2004), "Wavelet support vector machine", *IEEE Trans. Syst. Man Cybern. B.*, **34**(1), 34-39.

CC